



THE UNIVERSITY *of* EDINBURGH

## Edinburgh Research Explorer

### Tandem amplification of SCCmec can drive high level methicillin resistance in MRSA

**Citation for published version:**

Gallagher, LA, Coughlan, S, Black, NS, Lalor, P, Waters, EM, Wee, B, Watson, M, Downing, T, Fitzgerald, JR, Fleming, GTA & O'gara, JP 2017, 'Tandem amplification of SCCmec can drive high level methicillin resistance in MRSA', *Antimicrobial Agents and Chemotherapy*, vol. 61, no. 9, e00869-17.  
<https://doi.org/10.1128/AAC.00869-17>

**Digital Object Identifier (DOI):**

[10.1128/AAC.00869-17](https://doi.org/10.1128/AAC.00869-17)

**Link:**

[Link to publication record in Edinburgh Research Explorer](#)

**Document Version:**

Peer reviewed version

**Published In:**

Antimicrobial Agents and Chemotherapy

**General rights**

Copyright for the publications made accessible via the Edinburgh Research Explorer is retained by the author(s) and / or other copyright owners and it is a condition of accessing these publications that users recognise and abide by the legal requirements associated with these rights.

**Take down policy**

The University of Edinburgh has made every reasonable effort to ensure that Edinburgh Research Explorer content complies with UK legislation. If you believe that the public display of this file breaches copyright please contact [openaccess@ed.ac.uk](mailto:openaccess@ed.ac.uk) providing details, and we will remove access to the work immediately and investigate your claim.



1 AAC00869-17 REVISED

2

3 Tandem amplification of SCCmec can drive high level methicillin resistance in MRSA

4

5 Laura A. Gallagher<sup>1</sup>, Simone Coughlan<sup>2,3</sup>, Nikki S. Black<sup>1</sup>, Pierce Lalor<sup>1</sup>, Elaine M. Waters<sup>1</sup>,  
6 Bryan Wee<sup>2</sup>, Mick Watson<sup>2</sup>, Tim Downing<sup>3</sup>, J. Ross Fitzgerald<sup>2</sup>, Gerard T. A. Fleming<sup>1\*</sup> and  
7 James P. O’Gara<sup>1\*</sup>

8

9 <sup>1</sup>Department of Microbiology, School of Natural Sciences, National University of Ireland,  
10 Galway, Ireland.

11 <sup>2</sup>School of Mathematics, Statistics and Applied Mathematics, National University of Ireland,  
12 Galway, Ireland.

13 <sup>3</sup>School of Biotechnology, Dublin City University, Dublin 9, Ireland.

14 <sup>4</sup>Roslin Institute, The University of Edinburgh, Scotland, UK.

15

16 \*Correspondence:

17 James P. O’Gara: [jamesp.ogara@nuigalway.ie](mailto:jamesp.ogara@nuigalway.ie)

18 Gerard T. A. Fleming: [gerard.fleming@nuigalway.ie](mailto:gerard.fleming@nuigalway.ie)

19

20 Key words: *Staphylococcus*; SCCmec; beta-lactam; antibiotic; resistance; mechanism

21

22 **Running title:** Amplification of SCCmec is a new mechanism of high level  $\beta$ -lactam resistance  
23 in MRSA

24 **Abstract.** Hospital-associated methicillin-resistant *Staphylococcus aureus* strains typically  
25 express high level, homogenous (HoR)  $\beta$ -lactam resistance, whereas community-associated  
26 MRSA (CA-MRSA) more commonly express low level heterogeneous (HeR) resistance.  
27 Expression of the HoR phenotype typically requires both increased expression of  
28 the *mecA* gene, carried on the *Staphylococcus* cassette chromosome *SCCmec* element, and  
29 additional mutational event(s) elsewhere on the chromosome. Here the oxacillin  
30 concentration in a chemostat culture of the CA-MRSA strain USA300 was increased from 8  
31  $\mu\text{g/ml}$  to 130  $\mu\text{g/ml}$  over 13 days to isolate highly oxacillin resistant derivatives. A stable,  
32 small colony variant, designated HoR34, which had become established in the chemostat  
33 culture was found to have acquired mutations in *gdpP*, *clpX*, *guaA* and *camS*. Closer  
34 inspection of the genome sequence data further revealed that reads covering *SCCmec* were  
35  $\sim 10$  times over-represented compared to other parts of the chromosome. qPCR confirmed  
36  $>10$ -fold higher levels of *mecA* DNA on the HoR34 chromosome, and MinION genome  
37 sequencing verified the presence of 10 tandem repeats of the *SCCmec* element. qPCR  
38 further demonstrated that sub-culture of HoR34 in varying concentrations of oxacillin (0–  
39 100  $\mu\text{g/ml}$ ) was accompanied by accordion-like contraction and amplification of the *SCCmec*  
40 element. Although slower growing than USA300, HoR34 out-competed the parent strain in  
41 the presence of sub-inhibitory oxacillin. These data identify tandem amplification of the  
42 *SCCmec* element as a new mechanism of high-level methicillin resistance in MRSA, which  
43 may provide a competitive advantage for MRSA under antibiotic selection.

44

45 **Introduction**

46 In recent decades, the overall incidence of methicillin resistant *Staphylococcus aureus*  
47 infections has greatly increased due to the emergence of community-associated MRSA (CA-  
48 MRSA), which are increasingly displacing hospital associated-MRSA (HA-MRSA) strains in  
49 healthcare settings (1). Methicillin resistance is mediated by the *mecA*-encoded low affinity  
50 penicillin binding protein 2a carried on the mobile *Staphylococcus* cassette chromosome  
51 *mec* element (SCC*mec*). Heterogeneity is a feature of *S. aureus* methicillin resistance (2). In  
52 general clinical CA-MRSA isolates exhibit low level, heterogeneous methicillin resistance  
53 (HeR) under laboratory growth conditions, whereas HA-MRSA isolates can exhibit high-level,  
54 homogeneous methicillin resistance (HoR). HeR strains can express a HoR phenotype after  
55 selection on elevated concentrations of  $\beta$ -lactam antibiotics, via mechanism(s) involving the  
56 stringent response and altered c-di-AMP signalling (2).

57 In general, the capacity of pathogens like MRSA to become resistant to new drugs only  
58 becomes apparent months or years after their introduction into clinical practice, during  
59 which time exposure of the pathogen to new drugs gradually increases, as does the  
60 likelihood that endogenous resistance will emerge. This clinical scenario can be mimicked in  
61 the laboratory using standard, batch culture techniques to isolate bacterial mutants  
62 exhibiting resistance to an antimicrobial drug. However, such artificial culture conditions can  
63 mask the impact of acquired antimicrobial resistance (AMR) on bacterial fitness (3, 4), a  
64 phenomenon that plays a significant role in determining maintenance and spread of the  
65 AMR genotype in natural bacterial populations, and affects the disease-causing capacity of  
66 the pathogen. Here we used a continuous-growth chemostat to address this limitation by  
67 creating a more dynamic and competitive environment from which to isolate  
68 physiologically-relevant  $\beta$ -lactam resistant mutants. A USA300 culture was exposed to

69 increasing concentrations of oxacillin (8-130  $\mu\text{g/ml}$ ) over a thirteen-day period. Among the  
70 hyper-resistant mutants isolated was a stable small colony variant in which the tandem  
71 amplification of the *SCCmec* element was identified as a new mechanism of high-level  $\beta$ -  
72 lactam resistance in MRSA.

73 **Results and discussion**

74 **Isolation of USA300 oxacillin hyper-resistant mutants.** A USA300 nutrient broth culture was  
75 grown in a chemostat for 13 days. A sub-MIC concentration of oxacillin was used at the start  
76 of the chemostat culture and increased on an incremental, daily basis up to 130 µg/ml  
77 (equivalent to 800 µg/ml on Mueller Hinton, BHI or nutrient agar), as described in the  
78 methods. Isolated hyper resistant mutants were readily differentiated into i) white coloured  
79 small colony variants and ii) regular-sized, pigmented colonies (Fig. 1A). Using population  
80 analysis profiling as described previously (5), all the mutants were shown to be  
81 homogeneously resistant (HoR) (data not shown) and exhibited oxacillin MICs = 800 µg/ml.  
82 Further analysis revealed that the small colony mutants appeared to be phenotypically  
83 similar, exhibiting the same biofilm forming capacity and repressed β-haemolysis (data not  
84 shown). In contrast the faster growing HoR mutants appeared to be heterogeneous,  
85 exhibiting different levels of biofilm forming capacity and β-haemolytic activity on sheep  
86 blood agar (data not shown). Whole genome sequencing further revealed a variety of  
87 different mutations in nine HoR mutants recovered from the chemostat (Table 1). These  
88 included four mutants with Ser<sub>67</sub>Lys amino acid substitutions in DacA, the diadenylate  
89 cyclase responsible for synthesis of c-di-AMP, which has previously been implicated in  
90 the HoR phenotype (2, 6, 7), four mutants with five different mutations in genes  
91 encoding predicted lipoproteins and one mutant with a Glu<sub>227</sub>Gln substitution in a  
92 predicted ABC transporter designated *abcA* (8). Mutation of the *abcA* gene has  
93 previously been shown to increase β-lactam resistance and is associated with  
94 upregulation of the adjacent *pbpD* gene, which encodes penicillin binding protein 4 (8).

95 In addition to a small colony size (Fig. 1A), impaired growth (Fig. 1B) and expression of  
96 hyper-resistance to oxacillin, a representative SCV HoR, designated HoR34, also exhibited  
97 altered cell morphology including defective septa formation (Fig. 1C) and an approximately  
98 2-fold increase in cell wall thickness ( $18.6 \pm 1.8$  nm in USA300 versus  $36.1 \pm 4.2$  nm in  
99 HoR34)(Fig. 1D). Whole genome sequence analysis of HoR34 and the parent USA300 strain  
100 compared to the publically-available USA300 FPR3757 genome, revealed that plasmid  
101 pUSA02 (which carries tetracycline resistance) had been lost and identified non-  
102 synonymous mutations in the *gdpP* (c-di-AMP phosphodiesterase (2, 7)), *guaA* (GMP  
103 synthetase (9)), *clpX* (chaperone protein (10)) and *camS* (membrane lipoprotein (11)) genes  
104 (Table 1). GdpP is an c-di-AMP phosphodiesterase responsible for turnover of c-di-AMP  
105 synthesised by DacA, and has previously been implicated in the HoR phenotype (2, 7) but  
106 not a small colony phenotype, which is clinically important in persistent infections (12).  
107 Therefore to determine if the *guaA*, *clpX* or *camS* mutations (alone or in combination) were  
108 involved in the small colony size of HoR34, the mutant was subjected to daily subculture in  
109 the absence of antibiotic selection for 2 weeks in an effort to isolate fast-growing  
110 revertants. The SCV phenotype of HoR34 was stable and no fast growing revertants were  
111 isolated even after repeated attempts. However the oxacillin MIC of the passaged HoR34  
112 strain, designated HoR34p, was reduced from 800  $\mu\text{g/ml}$  to 300  $\mu\text{g/ml}$ , indicating that  
113 although the strain continued to be hyper-resistant, oxacillin resistance levels in this strain  
114 can be regulated.

115 To further tease out the contributions of the *guaA*, *clpX*, *camS* and *gdpP* mutations to the  
116 HoR34 phenotypes, wild type alleles of the four genes, including their upstream promoter  
117 sequences, were cloned on the medium copy number *E. coli-Staphylococcus* shuttle plasmid  
118 pLI50 and introduced into HoR34. The multicopy *clpX* plasmid was unstable in HoR34 and

119 rapidly lost in the absence of antibiotic selection. Furthermore imposition of continuous  
120 antibiotic selection for the *pcpX* plasmid in HoR34 appeared to be accompanied by the  
121 selection of compensatory mutations, as evidenced by the rapid emergence of fast growing  
122 colonies among the HoR34 small colony variants. Although we were unable to progress this  
123 complementation experiment further, two previous studies have shown that mutation of  
124 *clpX* is associated with increased resistance to  $\beta$ -lactam antibiotics (albeit not to the levels  
125 measured in HoR34) (10, 13), suggesting that the *clpX* mutation may contribute in part to  
126 increased oxacillin resistance in HoR34. The remaining complementation experiments  
127 revealed that neither *gdpP*, nor the *camS* and *guaA* genes had any significant effect on the  
128 colony morphology (data not shown) or oxacillin MIC of HoR34, as measured by Etest (Fig.  
129 2A) and agar dilutions (data not shown). Furthermore, the doubling times for HoR34 (31.9  
130 min), HoR34 *pguaA* (33.0 min), HoR34 *pgdpP* (31.7 min) and HoR34 *pcamS* (28.9 min) were  
131 all substantially slower than USA300 (22.6 min) and HoR34 grown in Ox 0.5  $\mu$ g/ml (32.70  
132 min), but not significantly different from each other indicating that the *guaA*, *camS* and  
133 *gdpP* mutations alone did not affect growth rate. Because GdpP and c-di-AMP signalling also  
134 contributes to the regulation of autolytic activity (2, 14), we further investigated this  
135 phenotype. Consistent with previous studies, the *gdpP* mutation in HoR34 was associated  
136 with increased autolytic activity that was successfully complemented only by *gdpP* and not  
137 *camS* or *guaA* (Fig. 2B). The potential roles of the identified mutations in *guaA*, *clpX* and  
138 *camS* in the HoR phenotype remain unclear but they may have emerged initially to support  
139 growth or maintain fitness at relatively lower oxacillin concentrations during the early  
140 stages of growth in the chemostat. It seems unlikely that the mutations in *camS*, *clpX* or  
141 *guaA* are accompanied by any gain of function; the *clpX* and *camS* genes contain mutations  
142 introducing stop codons (Table 1), while predicted loss of function mutations in *guaA* have



143 previously been implicated in the HoR phenotype (7). Taken together, these data suggest  
144 that the mutations in *guaA*, *clpX*, *camS* and *gdpP*, at least on their own, are not responsible  
145 for the HoR34 oxacillin hyper-resistance phenotype, and raised the possibility that other  
146 genomic rearrangements were responsible for this phenotype.

147 **Chromosomal amplification of the SCCmec element in HoR34.** A number of recent studies  
148 have indicated that large regions of the *S. aureus* chromosome can undergo duplication and  
149 amplification events (15, 16). To investigate if such genomic rearrangements had taken  
150 place in HoR34, read coverage across the genome was analysed. Illumina sequence reads  
151 covering the SCCmec element were >10 times over-represented compared to other parts of  
152 the chromosome (Fig. 3). LightCycler qPCR confirmed 10-fold higher levels of *mecA* in HoR34  
153 gDNA samples compared to USA300 (data not shown). To determine whether the SCCmec  
154 element had amplified on the chromosome or excised and re-integrated at multiple sites  
155 around the chromosome, we attempted to assemble the Illumina sequence reads  
156 corresponding to the SCCmec element into contigs. However these efforts were hampered  
157 by the short reads. To address this we re-sequenced the HoR34 genome using MinION  
158 technology, which generates sequence reads of 10Kb onto which the Illumina sequence  
159 reads were mapped. The combined MinION/Illumina sequence data revealed the presence  
160 of 10 tandem SCCmec element repeats on the HoR34 chromosome (Fig. 4). All 10 copies of  
161 SCCmec were completely intact and no additional DNA sequences were identified at the join  
162 sites. Oligonucleotide primers designed to span the join sites of tandem SCCmec elements  
163 amplified PCR produced of the predicted size from HoR34 but not USA300, whereas control  
164 primers targeting *mecA* amplified PCR products of the predicted size from both HoR34 and  
165 USA300 (Fig. 5A).

166 **Stability of the SCCmec amplification event.** The reduction in oxacillin MIC in the HoR34  
167 strain passaged in BHI media (from 800 to 300 µg/ml) indicated that the amplified SCCmec  
168 elements may be unstable in the absence of antibiotic selection. To measure SCCmec copy  
169 number, LightCycler qPCR was used to compare the relative abundance of *mecA* in HoR34  
170 grown in the presence and absence of oxacillin. These experiments revealed that the *mecA*  
171 copy number in the HoR34p strain that had been passaged daily in antibiotic-free BHI media  
172 for 2 weeks (oxacillin MIC = 300 µg/ml), was only 3-fold higher than USA300 (Fig. 5B),  
173 indicating that up to seven of the amplified SCCmec elements were excised/lost from the  
174 original chemostat isolate during this time. Interestingly the doubling time of HoR34p (32.70  
175 min) was not significantly different to that of HoR34 (31.9 min), indicating that a reduction  
176 in the number of amplified SCCmec elements was not sufficient to alleviate the growth  
177 defect. However further passage of HoR34p in 0.5, 64 and 100µg/ml oxacillin was  
178 accompanied by a significant, concentration-dependent increase in *mecA* copy numbers (up  
179 to 17-fold compared to USA300)(Fig. 5B), and an increase in MIC to ≥800 µg/ml. PCR  
180 amplification and sequencing was used to confirm that the identified mutations in the *guaA*,  
181 *gdpP*, *clpX* and *camS* genes of HoR34 had not reverted to wild type following passage in  
182 antibiotic free media (data not shown). These data suggest that recombination between the  
183 tandem SCCmec elements in HoR34 facilitates accordion-like contraction and expansion in  
184 response to oxacillin exposure. Consistent with these qPCR data, Western blot analysis of  
185 HoR34 grown in 0, 0.5, 64 and 100 µg/ml oxacillin also revealed concentration-dependent  
186 increases in PBP2a expression (Fig. 5C).

187 To investigate why a small colony variant may have been selected and maintained in the  
188 chemostat, we performed competition experiments between USA300 and HoR34.  
189 Predictably USA300 out-competed the slower-growing HoR34 in the absence of antibiotic

190 selection (Fig. 5D). However in the presence of sub-inhibitory oxacillin (0.5 µg/ml), HoR34  
191 strongly outcompeted the wild type (Fig. 5D). Collectively these data identify tandem  
192 amplification of the *SCCmec* element as a new mechanism of high-level methicillin  
193 resistance in MRSA, which may provide a competitive advantage for MRSA under antibiotic  
194 selection.

195 **Concluding remarks.** Several genetic mechanisms may have contributed alone or in  
196 combination to the *SCCmec* amplification event in HoR34. Expression of the *ccr* recombinase  
197 genes which excise *SCCmec* (17) can be increased by β-lactams and vancomycin (18),  
198 potentially generating multiple, extrachromosomal copies of *SCCmec* capable of subsequent  
199 reintegration. This possibility is supported by a recent study which identified a replication  
200 initiator gene upstream of the *ccr* recombinase genes suggesting that the element may be  
201 replicative (19). Other mechanisms that may have contributed to the *SCCmec* amplification,  
202 alone or in combination with Ccr-mediated excision, include RecA-dependent non-equal  
203 homologous recombination or RecA-independent mechanisms such as recombination  
204 between single-stranded repetitive sequence on sister chromatids at the replication fork  
205 (20). The absence of repeat sequences flanking the *SCCmec* amplification may also suggest  
206 that an initial double-strand break (DSB), followed by RecA-dependent DSB repair during  
207 rolling circle replication may drive the production of long tandem arrays in a single  
208 generation, which have previously been implicated in fast adaption to drug treatment (21).  
209 Following the initial *SCCmec* duplication/amplification, the long stretches of homology are  
210 likely to facilitate RecA-mediated expansion and contraction of the element in different  
211 concentrations of oxacillin, as recently observed in a *S. lugdenensis* strain carrying an  
212 amplified *isd* locus (16). Recombination events leading to partial deletion of the *SCCmec*  
213 locus have been described previously. For instance, increased vancomycin resistance has

214 been linked to site-specific insertion sequence-mediated excision of *SCCmec* (22), suggesting  
215 that distinct RecA-independent mechanisms may favour high or low copy numbers of *mecA*  
216 in high  $\beta$ -lactam or vancomycin environments, respectively.

217 Even though multiple copies of *SCCmec* were maintained by HoR34 following repeated  
218 subculture in the absence of oxacillin selection, no evidence for *SCCmec* amplification was  
219 found in a search of 404 MRSA genomes using read coverage of the *mecA* gene normalised  
220 with read coverage of three single copy genes (data not shown). The clinical relevance of  
221 this data merits further investigation, particularly given that  $\beta$ -lactams are not typically part  
222 of the treatment regimen for MRSA infections. However, this may change in view of ongoing  
223 clinical trials showing the therapeutic value of combining flucloxacillin and vancomycin for  
224 the treatment of MRSA sepsis (23, 24). Our growth competition experiments revealed the  
225 increased competitiveness of HoR34 in the presence of oxacillin was balanced by a  
226 significant loss of competitiveness in the absence of antibiotic selection, suggesting that  
227 MRSA strains carrying multiple *SCCmec* elements are unlikely to be maintained under  
228 physiological conditions or in clinical environments where exposure to antibiotics is  
229 sporadic. Taken together our data identify chromosomal amplification of the *SCCmec*  
230 element as a new mechanism that may be used by MRSA to adapt to, and be more  
231 competitive in, high oxacillin environments.

## 232 **Materials and Methods**

233 **Strains and culture conditions.** Strains used in this study are listed in Table 2 and were  
234 grown at 37°C in LB (Sigma), BHI (Oxoid), Mueller Hinton (Oxoid) or nutrient (Oxoid) broth  
235 supplemented with ampicillin (50 µg/ml), oxacillin (0.5, 64, 100 or 130 µg/ml),  
236 chloramphenicol (10 µg/ml) or erythromycin (10 µg/ml) as indicated. *S. aureus* strains were  
237 also grown on BHI agar media plates supplemented with oxacillin concentrations up to 1200  
238 µg/ml.

239  
240 **Measurement of oxacillin minimum inhibitory concentration (MIC).** The oxacillin MIC for  
241 the *S. aureus* strains used in this study was determined in accordance with the Clinical  
242 Laboratory Standards Institute (CLSI) guidelines and using E-tests strips from Biomerieux on  
243 Mueller Hinton agar (Oxoid) containing 2% NaCl.

244  
245 **Isolation of USA300 oxacillin hyper-resistant mutants using chemostat system.** The  
246 community-associated CA-MRSA strain, USA300 FPR3757, which expresses a HeR  
247 phenotype with an oxacillin minimum inhibitory concentration (MIC) on brain heart infusion  
248 or nutrient agar of 32 µg/ml was used in this study. A 580 ml capacity laboratory reactor  
249 containing 500 ml of nutrient broth (Oxoid) was used as described previously (25). USA300  
250 was inoculated into the chemostat and allowed to grow to stationary phase for 2 days at  
251 37°C in the absence of any antibiotic selection or media replacement. A growth media  
252 reservoir containing 20 l of nutrient broth was then connected to the chemostat and fed to  
253 the chemostat using a peristaltic pump at a flow rate of 100 ml/h, replacing the entire  
254 nutrient broth volume of the chemostat every 5h. After 24 hours continuous culture growth  
255 in the absence of antibiotic selection, the nutrient broth in the feeding tank was  
256 supplemented with oxacillin at a concentration of 8 mg/l. Thereafter the oxacillin  
257 concentration in the growth medium reservoir was increased in a step-wise manner every  
258 day reaching a final concentration of 130 mg/l on Day 12. Culture samples were collected  
259 aseptically from the chemostat after 24 hours culture at each oxacillin concentration before  
260 being serially diluted and inoculated onto BHI agar supplemented with oxacillin 100 µg/ml.  
261 The MICs of colonies recovered from these plates were determined on BHI agar  
262 supplemented with oxacillin ranging from 100-1000 µg/ml. All isolates examined were

263 hyper-resistant and capable of robust growth on BHI agar supplemented with 800 µg/ml  
264 oxacillin. Phenotypic and whole genome sequence analysis of the hyper-resistant mutants is  
265 described in the supplementary methods.

266

267 **Haemolysis, biofilm and autolysis assays.** Beta haemolysis was assessed on BHI agar  
268 supplemented with 5% sheep blood following overnight growth at 37°C and a further 24  
269 hours at 4°C. Semi-quantitative measurements of biofilm formation were determined under  
270 static conditions using Nunclon Hydrophilic tissue culture treated 96 well polystyrene plates  
271 (Nunc, Denmark) as described previously (26). Triton X-100 induced autolysis was measured  
272 essentially as described previously (27). Each experiment was repeated at least three times  
273 and average data presented.

274

275 **Transmission Electron Microscopy (TEM).** Overnight BHI cultures were diluted 1:200 in  
276 fresh BHI and grown at 37°C to an  $A_{600} = 1.0$ . 10 ml culture aliquots were subjected to  
277 centrifugation at  $8,000 \times g$ , and the cell pellets were re-suspended in fixation solution (2.5%  
278 glutaraldehyde in 0.1 M cacodylate buffer [pH 7.4]) and incubated overnight at 4°C. The  
279 fixed cells were further treated with 2% osmium tetroxide, followed by 0.25% uranyl acetate  
280 for contrast enhancement. The pellets were then dehydrated in increasing concentrations  
281 of ethanol as described above for the SEM cell preparation, followed by pure propylene  
282 oxide, and transferred to a series of resin and propylene oxide mixtures (50:50, 75:25, pure  
283 resin) before being embedded in Epon resin. Thin sections were cut on an ultramicrotome.  
284 Images were analysed using AMT v.542 software using a Hitachi H7000 instrument. At least  
285 3 to 5 measurements of cell wall thickness were performed on each cell and 88 cells were  
286 measured for each sample.

287

288 **PCR and Quantitative PCR.** Amplification of the *mecA* gene and the *SCCmec* junctions in  
289 HoR34 was achieved using the following primers (Table 3): *mecA*\_Fwd and *mecA*\_Rev (for  
290 *mecA*) and *SCCmecJNFwd* and *SCCmecJnRev* (for the *SCCmec* junctions). Quantitative PCR  
291 (qPCR) for *mecA* was performed on the Roche LightCycler 480 instrument using the  
292 LightCycler 480 Sybr Green Kit (Roche) and the following primers: *mecA1*\_Fwd and  
293 *mecA2*\_Rev. Cycling conditions were 95 °C for 5 minutes and followed by 45 cycles of 95 °C  
294 for 10 seconds, 58 °C for 20 seconds and 72°C for 20 seconds. Melt curve analysis was

performed at 95 °C for 5 seconds followed by 65 °C for one minute up to 97 °C at a ramp rate of 0.11c/sec with five readings taken for every degree of temperature increase. The *gyrB* gene was used as an internal standard for all reactions using previous described primers (2). For each reaction, the ratio of *mecA* and *gyrB* transcript number was calculated as follows:  $2^{(Ct_{gyrB} - Ct_{mecA})}$ . Each qPCR experiment was performed at least three times and average data and standard errors are presented.

**Analysis of PBP2a expression:** Total cell protein preparations were prepared from overnight cultures grown in 0, 0.5, 64 or 100 µg/ml oxacillin. Cell pellets were re-suspended in distilled water containing 5 µg/ml lysostaphin, 10 units of DNase I, and 50 µl of 10% SDS before being incubated at 37°C for 30 minutes. Insoluble material was pelleted by centrifugation and the supernatant used for Western blotting. Protein concentration was assessed using the Pierce BCA protein assay kit (Thermo Scientific). Protein samples were separated on a 10% SDS gel (Thermo Scientific) and transferred to nitrocellulose membranes (Thermo Scientific) using a TE 70 semidry transfer unit (Amersham). Anti-PBP2a antibodies (Abnova) were used at a 1:2000 dilution. A 1:200 dilution of protein G-horseradish peroxidase (HRP) conjugate (Sigma) was used to detect bound antibody and visualisation was achieved using a colorimetric detection system (Bio-Rad).

**Complementation of HoR34 with *gdpP*, *guaA*, *camS* and *clpX*.** The *gdpP*, *guaA*, *camS* and *clpX* genes were amplified from USA300 genomic DNA by PCR using primers listed in Table 2, before being cloned into the cloning vector pDrive (Quigen) in *Escherichia coli* TOP10. The sequence of inserts in recombinant plasmids was verified by Sanger sequencing (Source Biosciences) before being subcloned on *EcoRI* or *BamHI/HindIII* restriction fragments into the *E. coli* - *Staphylococcus* shuttle plasmid pLI50. The plasmids were transformed by electroporation into the restriction-deficient strain RN4220, and subsequently into HoR34. All plasmid-harboring strains were cultured in medium supplemented with 100 µg/ml ampicillin (*E. coli*) or 10 µg/ml chloramphenicol (*S. aureus*) for plasmid selection.

**Growth competition experiments.** Overnight cultures of USA300 and HoR34 cultures were diluted to  $A_{600} = 0.05$  in fresh BHI media and grown for 6h. The cell density of both exponential phase cultures was adjusted to  $A_{600} = 0.1$  in 500 ml flasks containing 50ml BHI or BHI supplemented with 0.5 µg/ml oxacillin and incubated at 37°C with shaking. The number



328 of colony forming units in samples collected at 0, 2, 4, 8, 24 and 48h was determined by  
329 plating serial dilutions on BHI agar. Colonies formed by each strain were readily  
330 differentiated based on their tetracycline resistance and appearance i.e. the HoR34 colonies  
331 were tetracycline sensitive and had a white-coloured, small colony phenotype whereas  
332 USA300 colonies were regular sized, tetracycline resistant and pigmented.

333

334 **Statistical analysis.** Two-tailed, two-sample equal variance Student's t-Tests were used to  
335 determine statistically significant differences in assays performed during this study. A *P*  
336 value <0.05 was deemed significant.

337

338 **Quality control of genome sequence data.** Read quality was assessed by screening the read  
339 length, nucleotide and quality score distributions using FastQC  
340 (<http://www.bioinformatics.babraham.ac.uk/projects/fastqc/>) and the FASTX-Toolkit  
341 ([http://hannonlab.cshl.edu/fastx\\_toolkit/index.html](http://hannonlab.cshl.edu/fastx_toolkit/index.html)). The DNA reads were trimmed based  
342 on quality scores. Potential adaptor sequence was removed using Trimmomatic v0.32 (28),  
343 which scanned reads using a four-base sliding window and trimmed reads where the  
344 average Phred base quality of the window was below 30. All ambiguous 'N' bases and reads  
345 shorter than 35 bp were removed. The first 20 bases of the DNA reads were removed  
346 because they had a nucleotide content that deviated from the expected 25% rate for each  
347 base. The DNA reads were corrected using BayesHammer (29) to reduce sequencing errors  
348 that can reduce the alignment quality, increase false positive SNP rates and reduce the  
349 number of valid SNPs (30). These steps retained 84% of the initial DNA reads among HoR  
350 isolates from the chemostat yielding median quality values > 30 across the reads. Insert  
351 sizes were an average of 185. Read lengths after trimming and filtering averaged 185 bp and  
352 the average coverage per sample on the chromosome, calculated using the Bedtools  
353 genomecov function (31) on mapped reads, ranged from 47 to 197.

354 **Genome assembly.** The error-corrected paired and unpaired reads for each DNA sample  
355 were assembled using SPAdes v3.1.1 [5] with k-mers 21, 33, 55, 77, 99 and 127 and the  
356 'careful' parameter, which minimized the number of mismatches in the contigs (32). The  
357 resulting assemblies were compared to the reference USA300\_FPR3757 (PMID:16517273)  
358 chromosome using QUAST v2.3 (33). The GC content of each assembly was 32.6%, and there



359 were between 31 and 51 scaffolds per assembly, with N50 values > 200 Kb. One or two  
360 short gaps (<500 bp) were found in each assembly that could not be fully closed using  
361 Gapfiller (34).

362 **Single nucleotide polymorphism (SNP) calling using assembly and read-mapping.** The  
363 chromosome and three plasmids (GenBank accessions NC\_007790-NC\_007793) were  
364 indexed with *k*-mer of thirteen and step size of two using SMALT v5.7  
365 (<http://www.sanger.ac.uk/science/tools/smalt-0>). The error-corrected DNA reads were  
366 mapped to the genome with SMALT, which applied a Smith-Waterman sequence alignment  
367 algorithm. The SAM (sequence alignment/map) files were converted to BAM (binary  
368 alignment/map) files using Samtools v0.1.18 (35). The BAM files were then coordinate-  
369 sorted, the paired and unpaired files were merged, and PCR duplicate reads were removed.  
370 Candidate SNPs were detected where the base quality (BQ) was >25, the mapping quality  
371 (MQ) was >30, and the read depth was <100 using Samtools Mpileup v0.1.18, Bcftools  
372 v0.1.17-dev, and the Samtools v0.1.11 vcfutils.pl function. The read depth allele frequency  
373 of the non-reference allele (RDAF) and local coverage were estimated using Samtools Pileup  
374 v0.1.11.

375 To call SNPs using an assembly-based approach, the scaffolds produced by SPAdes were  
376 aligned to the USA300 reference genome using nucmer in the MUMmer v3.23 package. This  
377 was followed by eliminating conflicting repeat copies using the 'delta-filter' command and  
378 the 'show-snps' comand to call SNPs and indels. The union of SNPs called by nucmer and  
379 SNPs called by Bcftools was used as a candidate SNP set. These sites were queried across all  
380 samples using the Samtools Pileup files to find false negative SNPs uncalled by nucmer or  
381 Bcftools. The RDAF of the non-reference alleles was reported for each SNP using Samtools  
382 Pileup output. Each candidate SNP was assessed using the following additional criteria:

383

- 384 1) SNP Quality (SQ) >30
- 385 2) read coverage >5
- 386 3) forward-reverse read coverage ratio between 0.1 and 0.9
- 387 4) non-reference read allele frequency >0.1
- 388 5) 2+ forward reads

389 6) 2+ reverse reads

390 Results were converted to variant call format (VCF) and annotated. SNPs were homozygous  
391 if the RDAF was  $\geq 0.85$  and heterozygous if  $0.1 < \text{RDAF} < 0.85$ . Insufficient read depth  
392 coverage was present to predict SNPs with  $\text{RDAF} < 0.1$ .

393 **Indel calling using split-read mapping.** Deletions and short insertions (indels) were called  
394 using the samtopindel script to convert the BAM files, and then with Pindel (36) to only keep  
395 indels with at least ten supporting reads. The RDAF of the indels smaller than the read  
396 length were calculated using the BAM files in IGV (number of reads with indel at locus / all  
397 reads at the locus). For indels greater than one bp in length, the sum of the number of reads  
398 with the indel was divided by the sum of the number of reads at each site in the indel. This  
399 approach may be limited by uneven coverage at a locus. If the indel was longer than the  
400 read length, then a lack of read coverage at the sites predicted to have the mutation was  
401 considered evidence of the deletion and the RDAF was set to one.

402 **Variant annotation.** The functional effect of SNPs and indels was estimated by annotation  
403 with SnpEff v4.0e (37) using the 'Staphylococcus\_aureus\_USA300\_FPR3757\_uid58555'  
404 database file from the SnpEff database. Results were manually checked using the reference  
405 genome annotation.

406 **Copy number variation detection using read coverage.** Copy number variants (CNVs) were  
407 screened using the BAM files containing reads with  $\text{MQ} > 30$  to reduce false positive rates  
408 [12–14]. Coverage was calculated for every base using genomecov in Bedtools with the '-d'  
409 flag (31) so that the median chromosomal coverage could be calculated for each sample.  
410 Genome-wide coverage levels were analysed in 10 Kb and 25 Kb windows and plotted as 5  
411 Kb sliding windows with a 2.5 Kb step using the Bedtools makewindows function (31).  
412 Coverage for each window was normalised by dividing it by the median coverage of the  
413 chromosome to produce a copy number estimate. Windows with copy number  $\geq 2$  were  
414 reported. The copy number of plasmids was determined by dividing the median read  
415 coverage of the plasmid by the median read coverage of the chromosome.

416 **MinION long-read genome sequencing.** To evaluate the number of SCCmec copies and their  
417 location contiguous with or excised from the chromosome, genomic DNA from HoR34 was

418 amplified to generate long reads using a Oxford Nanopore Technologies (ONT) MinION.  
419 MinION sequencing library construction was carried out according to manufacturer's  
420 instructions and as previously described (38). The library was sequenced on an R7.3 MinION  
421 flowcell using the 2D sequencing protocol. The run produced 26859 FAST5 files, which were  
422 processed using poRe (39), yielding 17254 2D reads. These reads were used with the MiSeq  
423 data in a hybrid assembly using SPAdes (32) and SSPACE-LongRead (40) to produce a single  
424 contig.

425

426

427

428 **Figure Legends**

429

430 **Figure 1. Growth and cell morphology phenotypes of USA300 and HoR34.** **A.** Small colony  
431 variants and other isolates recovered from the chemostat culture after 13 days at a final  
432 oxacillin concentration of 130 mg/l grown on BHI agar for 24 h. **B.** Growth curve of USA300  
433 and HoR34 grown for 20 hours in BHI media at 37°C with vigorous aeration. The number of  
434 colony forming units per ml in culture samples removed at regular intervals was determined  
435 by plating on BHI agar. **C.** Cell morphology of USA300 and HoR34 imaged using transmission  
436 electron microscopy (TEM) at 8,000× magnification. **D.** Cell wall thickness of USA300 and  
437 HoR34 determined using TEM at 100,000× magnification and AMT v.542 imaging software.

438

439 **Figure 2. Oxacillin susceptibility and autolysis phenotypes of USA300 and HoR34.** **A.**  
440 Oxacillin MIC of USA300, HoR34 and HoR34 carrying plasmids pLI50 (control), *pgdpP*, *pguaA*  
441 and *pcamS* determined using Etests. **B.** Autolytic activity in USA300 and HoR34. USA300,  
442 HoR34, HoR34 carrying plasmids pLI50 (control), *pgdpP*, *pguaA* and *pcamS*, and a USA300  
443 JE2 *atl* mutant (negative control) were grown to early exponential phase in BHI at 37°C and  
444 washed in PBS and adjusted to  $A_{600} = 1.0$  in 0.01% Triton X-100. The  $A_{600}$  was measured  
445 initially and at 15 min intervals thereafter with shaking incubation at 37°C. Autolytic activity  
446 is expressed as a percentage of the initial  $A_{600}$ . Average results from three independent  
447 experiments shown.

448

449 **Figure 3.** Copy number as determined by Illumina sequence read coverage across *SCCmec*  
450 for USA300 (Sample 1A\_S1), HoR34 (Sample 8A\_S8, highlighted with blue box) and eight  
451 other isolates from the chemostat culture. The position on the chromosome is indicated,  
452 with *SCCmec* coordinates between 0.034 and 0.057 Mb. The blue lines depict locally  
453 weighted scatterplot smoothing (lowess) applied to the data points (black). Note that the y-  
454 axis for HoR34 differs from the other samples.

455

456 **Figure 4.** Chromosomal organisation of HoR34 depicting expansion of the *SCCmec* element  
457 and locations of *gdpP*, *clpX*, *camS* and *guaA* mutations. On the circular map, the inner track  
458 shows copy number of 10 kb non-overlapping loci across the genome with loci that had  
459 copy number greater than two shown in red and those with copy number less than two

460 shown in blue. The next track shows black blocks illustrating different regions on the  
461 genome e.g. *SCCmec* and *ACME*. Single nucleotide polymorphisms are shown on the third  
462 track. Missense mutations are labelled in green whereas stop gain mutations are labelled in  
463 blue. Genes are shown in the outermost tracks. Genes transcribed in the forward (5' -> 3')  
464 direction are labelled in green and are in the outside track whereas those transcribed in the  
465 reverse direction are labelled in red.

466  
467 **Figure 5. Chromosomal amplification of *SCCmec* can drive high level oxacillin resistance. A.**

468 PCR amplification across the *SCCmec* junctions in HoR34. Amplification of the *mecA* gene in  
469 both USA300 and HoR34 was used as a control. **B.** Comparison of relative *mecA* abundance  
470 by LightCycler qPCR in USA300 and HoR34 grown for 24 h in BHI supplemented with 0, 0.5,  
471 64 or 100 mg/ml oxacillin. **C.** Comparison of relative PBP2a expression by Western blot  
472 analysis in USA300 and HoR34 grown in BHI and BHI supplemented with 0, 0.5, 64 or 100  
473 mg/ml oxacillin. **D.** Competitive growth of USA300 and HoR34 over 48 hours in BHI and BHI  
474 supplemented with oxacillin (0.5 mg/ml). The CFU of each strain was enumerated on BHI  
475 agar to count all bacteria and BHI oxacillin (30 mg/ml) to count HoR34. The ratio of the two  
476 strains in each culture is shown. The data presented are mean and SD of three experiments.  
477 Statistical evaluation was performed using a paired two tailed t-test.

478

479

480

481 **Acknowledgements.** This study was funded by grants from the Irish Health Research Board  
482 (HRA-POR-2012-51 and HRA-POR-2015-1158) (to J.P.O'G). We thank Cyril Carroll and Claire  
483 Fingleton for assistance with the chemostat experiment and analysis of HoR34.

484 **Table 1. Genetic alterations in USA300 oxacillin hyper-resistant mutants from the**  
 485 **chemostat culture**

Isolate, growth characteristic	Genome position	Nucleotide change	Amino acid change	Locus tag/gene
HoR20, fast-growing	703854	G-C	Glu <sub>227</sub> Gln	RS03375/ <i>abcA</i>
HoR18, 21, 27, 36; fast-growing	110748, 110752,111618, 111630, 111648	Multiple	Multiple	RS00520-RS00525 /uncharacterized lipoprotein genes
HoR33, 41, 43, 46; fast-growing	2288896	G-A	Ser <sub>67</sub> Lys	RS11640/ <i>dacA</i>
HoR34, slow-growing	19122	A-C	Thr <sub>260</sub> Pro	<i>gdpP</i> (c-di-AMP phosphodiesterase (14))
	44078	C-T	Ala <sub>314</sub> Val	<i>guaA</i> (GMP synthetase (9))
	441379	G-T	Glu <sub>511</sub> Asp	<i>guaA</i>
	1775825	C-A	Glu <sub>37</sub> STOP	<i>clpX</i> (Chaperone with ClpP- dependent role in protein degradation and ClpP-independent role in protein folding (10))
	2046530	G-A	Gln <sub>305</sub> STOP	<i>camS</i> (membrane lipoprotein involve in sex pheromone biosynthesis (11))

486

487

488 **Table 2. Bacterial strains and plasmids used in this study**

Strains/plasmids	Relevant Details
<b><i>S. aureus</i></b>	
RN4220	Restriction-deficient laboratory <i>S. aureus</i> .
USA300	CA-MRSA expressing heterogeneous resistance to oxacillin
HoR34	USA300 derivative expressing high level resistance to oxacillin
ATCC 29213	MSSA strain for susceptibility testing
JE2 <i>atl::erm</i>	Transposon mutation in the major autolysin gene <i>atl</i> of strain JE2, a USA300 derivative used in the construction of the Nebraska Transposon mutant library (41). Exhibits impaired autolytic activity.
<b><i>E. coli</i></b>	
<b>Plasmids</b>	
pLI50	<i>E. coli-Staphylococcus</i> shuttle vector. Ap <sup>r</sup> ( <i>E. coli</i> ), Cm <sup>r</sup> ( <i>Staphylococcus</i> ).
pDrive	<i>E. coli</i> cloning vector

489

490

491

492



493 **Table 3. Oligonucleotide primers used in this study**

Target Gene	Primer Name	Primer Sequence (5'-3')
<i>gdpP</i>	<i>gdpP_Fwd</i>	GCCGAATGCAGTAACGATTT
	<i>gdpP_Rev</i>	TTGTTGGCGTTCTTGTTTTG
<i>guaA</i>	<i>guaA_Fwd</i>	AGAGGACAAAGCGCCTAAGA
	<i>guaA_Rev</i>	CCTTACCCCTTTTCCGTCCT
<i>clpX</i>	<i>clpX_Fwd</i>	AACGCAAAGTTCGTTGAAGG
	<i>clpX_Rev</i>	TGAGCGTCAACTTTGATTGG
<i>camS</i>	<i>camS_Fwd</i>	GCTGGTGAAGATGCAGGTTT
	<i>camS_Rev</i>	CCTGGTGCATTTGTTGAACTG
<i>mecA</i>	<i>mecA_Fwd</i>	CATATCGTGAGCAATGAACTGA
	<i>mecA_Rev</i>	CATCGTTACGGATTGCTTCA
SCCmec Junction	SCCmecIn_Fwd	CTTGCTGGGTGCTATTTGA
	SCCmecIn_Rev	CGCTGTCTTCTGTATTTG
<i>mecA</i>	<i>mecA1_Fwd</i>	TGCTCAATATAAAATTAACAACTACGGTAAC
	<i>mecA1_Rev</i>	GAATAATGACGCTATGATCCCAA
<i>gyrB</i>	<i>gyrB_Fwd</i>	CCAGGTAAATTAGCCGATTGC
	<i>gyrB_Rev</i>	AAATCGCCTGCGTTCTAGAG

494

495

496 **References**

- 497 1. **Bal AM, Coombs GW, Holden MT, Lindsay JA, Nimmo GR, Tattevin P, Skov RL.** 2016.  
498 Genomic insights into the emergence and spread of international clones of  
499 healthcare-, community- and livestock-associated methicillin-resistant *Staphylococcus*  
500 *aureus*: Blurring of the traditional definitions. *J Glob Antimicrob Resist* **6**:95-101.
- 501 2. **Pozzi C, Waters EM, Rudkin JK, Schaeffer CR, Lohan AJ, Tong P, Loftus BJ, Pier GB,**  
502 **Fey PD, Massey RC, O'Gara JP.** 2012. Methicillin resistance alters the biofilm  
503 phenotype and attenuates virulence in *Staphylococcus aureus* device-associated  
504 infections. *PLoS Pathog* **8**:e1002626.
- 505 3. **Andersson DI, Levin BR.** 1999. The biological cost of antibiotic resistance. *Curr Opin*  
506 *Microbiol* **2**:489-493.
- 507 4. **Gagneux S, Long CD, Small PM, Van T, Schoolnik GK, Bohannon BJ.** 2006. The  
508 competitive cost of antibiotic resistance in *Mycobacterium tuberculosis*. *Science*  
509 **312**:1944-1946.
- 510 5. **Sieradzki K, Tomasz A.** 1997. Suppression of beta-lactam antibiotic resistance in a  
511 methicillin-resistant *Staphylococcus aureus* through synergic action of early cell wall  
512 inhibitors and some other antibiotics. *J Antimicrob Chemother* **39 Suppl A**:47-51.
- 513 6. **Dengler V, McCallum N, Kiefer P, Christen P, Patrignani A, Vorholt JA, Berger-Bachi**  
514 **B, Senn MM.** 2013. Mutation in the C-di-AMP cyclase *dacA* affects fitness and  
515 resistance of methicillin resistant *Staphylococcus aureus*. *PLoS One* **8**:e73512.
- 516 7. **Dordel J, Kim C, Chung M, Pardos de la Gandara M, Holden MT, Parkhill J, de**  
517 **Lencastre H, Bentley SD, Tomasz A.** 2014. Novel determinants of antibiotic  
518 resistance: identification of mutated loci in highly methicillin-resistant  
519 subpopulations of methicillin-resistant *Staphylococcus aureus*. *MBio* **5**:e01000.
- 520 8. **Domanski TL, de Jonge BL, Bayles KW.** 1997. Transcription analysis of the  
521 *Staphylococcus aureus* gene encoding penicillin-binding protein 4. *J Bacteriol*  
522 **179**:2651-2657.
- 523 9. **Mulhbacher J, Brouillette E, Allard M, Fortier LC, Malouin F, Lafontaine DA.** 2010.  
524 Novel riboswitch ligand analogs as selective inhibitors of guanine-related metabolic  
525 pathways. *PLoS Pathog* **6**:e1000865.
- 526 10. **Baek KT, Bowman L, Millership C, Dupont Sogaard M, Kaever V, Siljamaki P,**  
527 **Savijoki K, Varmanen P, Nyman TA, Grundling A, Frees D.** 2016. The Cell Wall  
528 Polymer Lipoteichoic Acid Becomes Nonessential in *Staphylococcus aureus* Cells  
529 Lacking the ClpX Chaperone. *MBio* **7**.
- 530 11. **Shahmirzadi SV, Nguyen MT, Gotz F.** 2016. Evaluation of *Staphylococcus aureus*  
531 Lipoproteins: Role in Nutritional Acquisition and Pathogenicity. *Front Microbiol*  
532 **7**:1404.
- 533 12. **Proctor RA, Kriegeskorte A, Kahl BC, Becker K, Loffler B, Peters G.** 2014.  
534 *Staphylococcus aureus* Small Colony Variants (SCVs): a road map for the metabolic  
535 pathways involved in persistent infections. *Front Cell Infect Microbiol* **4**:99.
- 536 13. **Baek KT, Grundling A, Mogensen RG, Thogersen L, Petersen A, Paulander W, Frees**  
537 **D.** 2014. beta-Lactam resistance in methicillin-resistant *Staphylococcus aureus*  
538 USA300 is increased by inactivation of the ClpXP protease. *Antimicrob Agents*  
539 *Chemother* **58**:4593-4603.

- 540 14. **Corrigan RM, Abbott JC, Burhenne H, Kaever V, Grundling A.** 2011. c-di-AMP is a  
541 new second messenger in *Staphylococcus aureus* with a role in controlling cell size  
542 and envelope stress. *PLoS Pathog* **7**:e1002217.
- 543 15. **Gao W, Monk IR, Tobias NJ, Gladman SL, Seemann T, Stinear TP, Howden BP.** 2015.  
544 Large tandem chromosome expansions facilitate niche adaptation during persistent  
545 infection with drug-resistant *Staphylococcus aureus*. *Microbial Genomics* **1**.
- 546 16. **Heilbronner S, Monk IR, Brozyna JR, Heinrichs DE, Skaar EP, Peschel A, Foster TJ.**  
547 2016. Competing for Iron: Duplication and Amplification of the *isd* Locus in  
548 *Staphylococcus lugdunensis* HKU09-01 Provides a Competitive Advantage to  
549 Overcome Nutritional Limitation. *PLoS Genet* **12**:e1006246.
- 550 17. **Diep BA, Stone GG, Basuino L, Graber CJ, Miller A, des Etages SA, Jones A,**  
551 **Palazzolo-Ballance AM, Perdreau-Remington F, Sensabaugh GF, DeLeo FR,**  
552 **Chambers HF.** 2008. The arginine catabolic mobile element and staphylococcal  
553 chromosomal cassette *mec* linkage: convergence of virulence and resistance in the  
554 USA300 clone of methicillin-resistant *Staphylococcus aureus*. *J Infect Dis* **197**:1523-  
555 1530.
- 556 18. **Higgins PG, Rosato AE, Seifert H, Archer GL, Wisplinghoff H.** 2009. Differential  
557 expression of *ccrA* in methicillin-resistant *Staphylococcus aureus* strains carrying  
558 staphylococcal cassette chromosome *mec* type II and IVa elements. *Antimicrob*  
559 *Agents Chemother* **53**:4556-4558.
- 560 19. **Mir-Sanchis I, Roman CA, Misiura A, Pigli YZ, Boyle-Vavra S, Rice PA.** 2016.  
561 Staphylococcal SCCmec elements encode an active MCM-like helicase and thus may  
562 be replicative. *Nat Struct Mol Biol* **23**:891-898.
- 563 20. **Lovett ST, Drapkin PT, Sutera VA, Jr., Gluckman-Peskind TJ.** 1993. A sister-strand  
564 exchange mechanism for *recA*-independent deletion of repeated DNA sequences in  
565 *Escherichia coli*. *Genetics* **135**:631-642.
- 566 21. **Sandegren L, Andersson DI.** 2009. Bacterial gene amplification: implications for the  
567 evolution of antibiotic resistance. *Nat Rev Microbiol* **7**:578-588.
- 568 22. **Noto MJ, Fox PM, Archer GL.** 2008. Spontaneous deletion of the methicillin  
569 resistance determinant, *mecA*, partially compensates for the fitness cost associated  
570 with high-level vancomycin resistance in *Staphylococcus aureus*. *Antimicrob Agents*  
571 *Chemother* **52**:1221-1229.
- 572 23. **Tong SY, Nelson J, Paterson DL, Fowler VG, Jr., Howden BP, Cheng AC, Chatfield M,**  
573 **Lipman J, Van Hal S, O'Sullivan M, Robinson JO, Yahav D, Lye D, Davis JS, group Cs,**  
574 **the Australasian Society for Infectious Diseases Clinical Research N.** 2016.  
575 CAMERA2 - combination antibiotic therapy for methicillin-resistant *Staphylococcus*  
576 *aureus* infection: study protocol for a randomised controlled trial. *Trials* **17**:170.
- 577 24. **Davis JS, Sud A, O'Sullivan MV, Robinson JO, Ferguson PE, Foo H, van Hal SJ, Ralph**  
578 **AP, Howden BP, Binks PM, Kirby A, Tong SY, Combination Antibiotics for MRSasg,**  
579 **Australasian Society for Infectious Diseases Clinical Research N.** 2016. Combination  
580 of Vancomycin and beta-Lactam Therapy for Methicillin-Resistant *Staphylococcus*  
581 *aureus* Bacteremia: A Pilot Multicenter Randomized Controlled Trial. *Clin Infect Dis*  
582 **62**:173-180.
- 583 25. **Fleming GTA, Patching JW.** 2008. *The Fermenter in Research and Development.*  
584 Wiley, Chichester, England.

- 585 26. **Conlon KM, Humphreys H, O'Gara JP.** 2002. *icaR* encodes a transcriptional repressor  
586 involved in environmental regulation of *ica* operon expression and biofilm formation  
587 in *Staphylococcus epidermidis*. *J Bacteriol* **184**:4400-4408.
- 588 27. **McCarthy H, Waters EM, Bose JL, Foster S, Bayles KW, O'Neill E, Fey PD, O'Gara JP.**  
589 2016. The major autolysin is redundant for *Staphylococcus aureus* USA300 LAC JE2  
590 virulence in a murine device-related infection model. *FEMS Microbiol Lett*  
591 **363**:fnw087.
- 592 28. **Bolger AM, Lohse M, Usadel B.** 2014. Trimmomatic: a flexible trimmer for Illumina  
593 sequence data. *Bioinformatics* **30**:2114-2120.
- 594 29. **Nikolenko SI, Korobeynikov AI, Alekseyev MA.** 2013. BayesHammer: Bayesian  
595 clustering for error correction in single-cell sequencing. *BMC Genomics* **14 Suppl**  
596 **1**:S7.
- 597 30. **Kelley DR, Schatz MC, Salzberg SL.** 2010. Quake: quality-aware detection and  
598 correction of sequencing errors. *Genome Biol* **11**:R116.
- 599 31. **Quinlan AR, Hall IM.** 2010. BEDTools: a flexible suite of utilities for comparing  
600 genomic features. *Bioinformatics* **26**:841-842.
- 601 32. **Bankevich A, Nurk S, Antipov D, Gurevich AA, Dvorkin M, Kulikov AS, Lesin VM,**  
602 **Nikolenko SI, Pham S, Prjibelski AD, Pyshkin AV, Sirotkin AV, Vyahhi N, Tesler G,**  
603 **Alekseyev MA, Pevzner PA.** 2012. SPAdes: a new genome assembly algorithm and  
604 its applications to single-cell sequencing. *J Comput Biol* **19**:455-477.
- 605 33. **Gurevich A, Saveliev V, Vyahhi N, Tesler G.** 2013. QUAST: quality assessment tool  
606 for genome assemblies. *Bioinformatics* **29**:1072-1075.
- 607 34. **Boetzer M, Pirovano W.** 2012. Toward almost closed genomes with GapFiller.  
608 *Genome Biol* **13**:R56.
- 609 35. **Li H, Handsaker B, Wysoker A, Fennell T, Ruan J, Homer N, Marth G, Abecasis G,**  
610 **Durbin R, Genome Project Data Processing S.** 2009. The Sequence Alignment/Map  
611 format and SAMtools. *Bioinformatics* **25**:2078-2079.
- 612 36. **Ye K, Schulz MH, Long Q, Apweiler R, Ning Z.** 2009. Pindel: a pattern growth  
613 approach to detect break points of large deletions and medium sized insertions from  
614 paired-end short reads. *Bioinformatics* **25**:2865-2871.
- 615 37. **Cingolani P, Platts A, Wang le L, Coon M, Nguyen T, Wang L, Land SJ, Lu X, Ruden**  
616 **DM.** 2012. A program for annotating and predicting the effects of single nucleotide  
617 polymorphisms, SnpEff: SNPs in the genome of *Drosophila melanogaster* strain  
618 w1118; iso-2; iso-3. *Fly (Austin)* **6**:80-92.
- 619 38. **Risse J, Thomson M, Patrick S, Blakely G, Koutsovoulos G, Blaxter M, Watson M.**  
620 2015. A single chromosome assembly of *Bacteroides fragilis* strain BE1 from Illumina  
621 and MinION nanopore sequencing data. *Gigascience* **4**:60.
- 622 39. **Watson M, Thomson M, Risse J, Talbot R, Santoyo-Lopez J, Gharbi K, Blaxter M.**  
623 2015. poRe: an R package for the visualization and analysis of nanopore sequencing  
624 data. *Bioinformatics* **31**:114-115.
- 625 40. **Boetzer M, Pirovano W.** 2014. SSPACE-LongRead: scaffolding bacterial draft  
626 genomes using long read sequence information. *BMC Bioinformatics* **15**:211.
- 627 41. **Fey PD, Endres JL, Yajjala VK, Widhelm TJ, Boissy RJ, Bose JL, Bayles KW.** 2013. A  
628 genetic resource for rapid and comprehensive phenotype screening of nonessential  
629 *Staphylococcus aureus* genes. *MBio* **4**:e00537-00512.

630

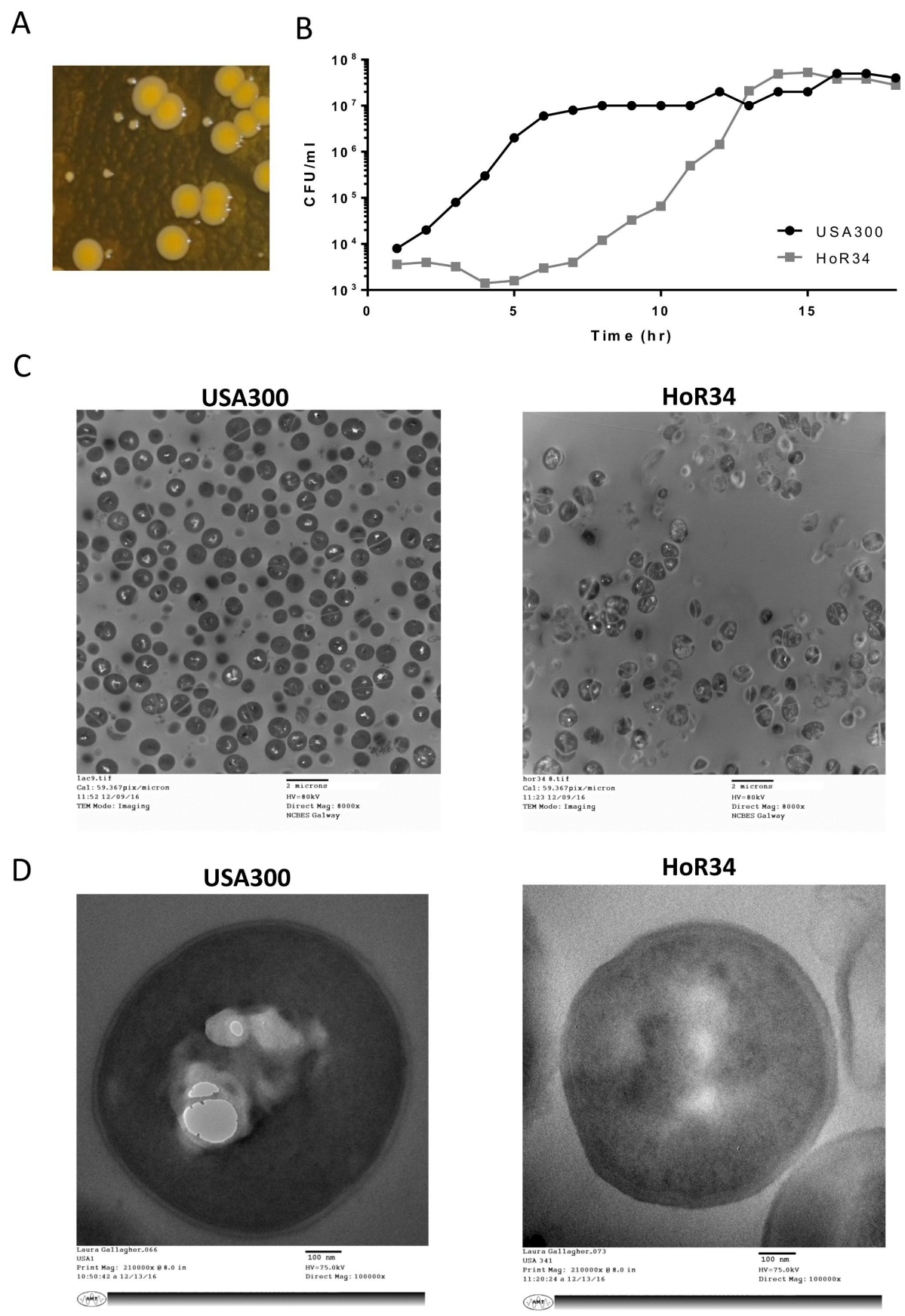


Fig. 1



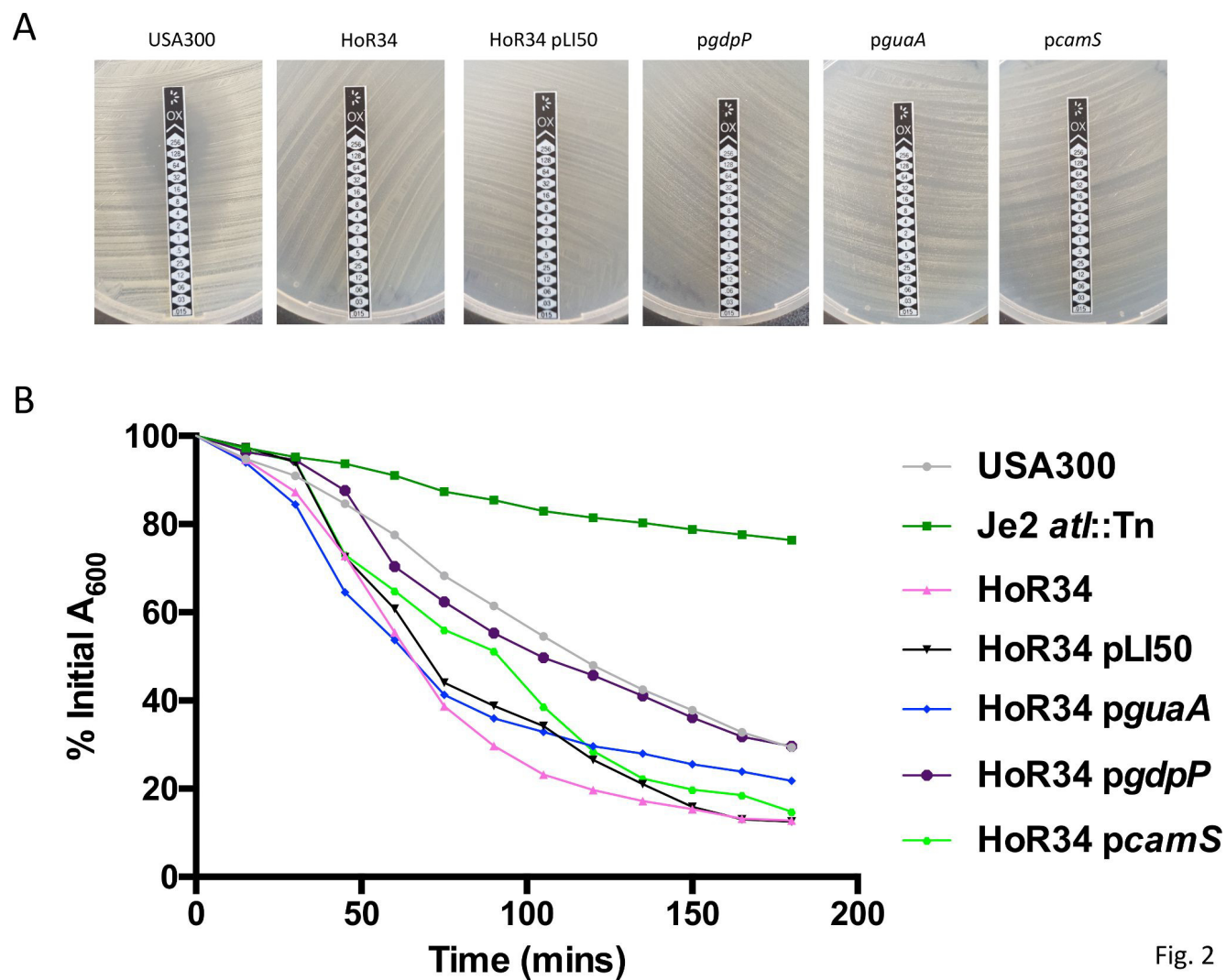


Fig. 2

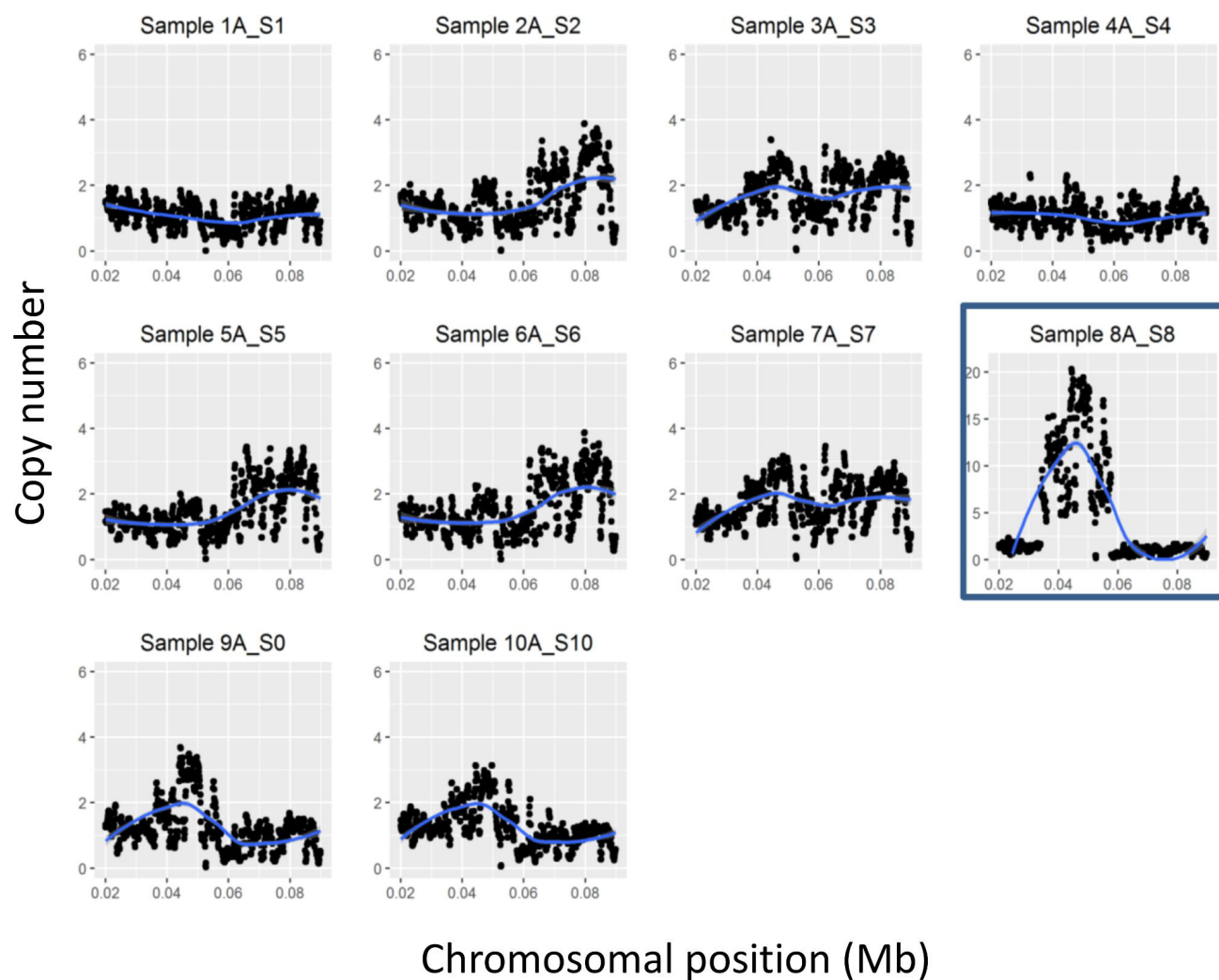


Fig. 3

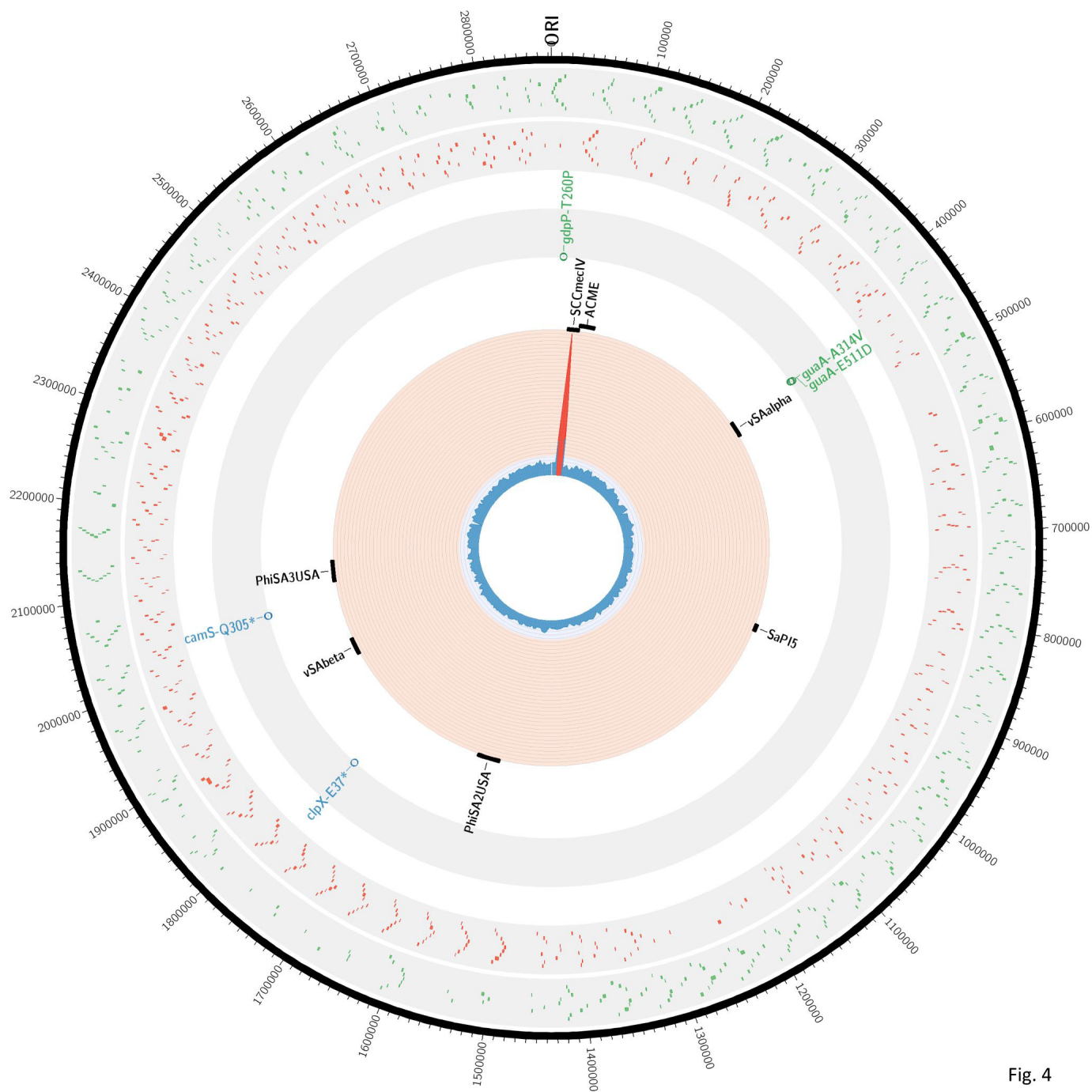


Fig. 4



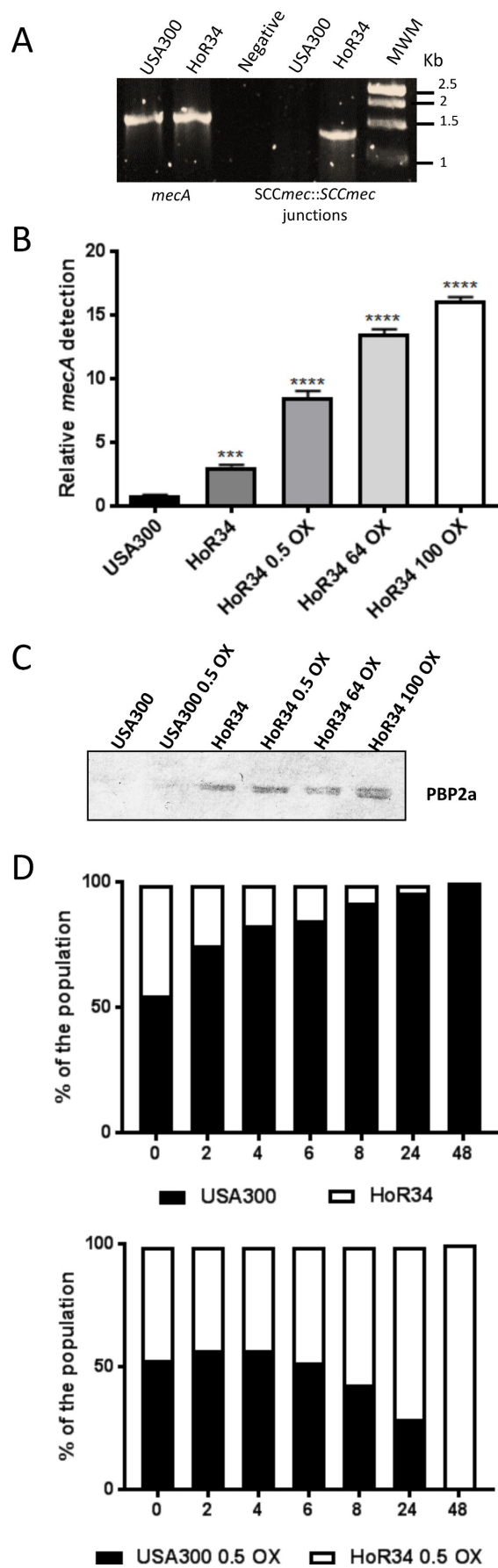


Fig. 5